

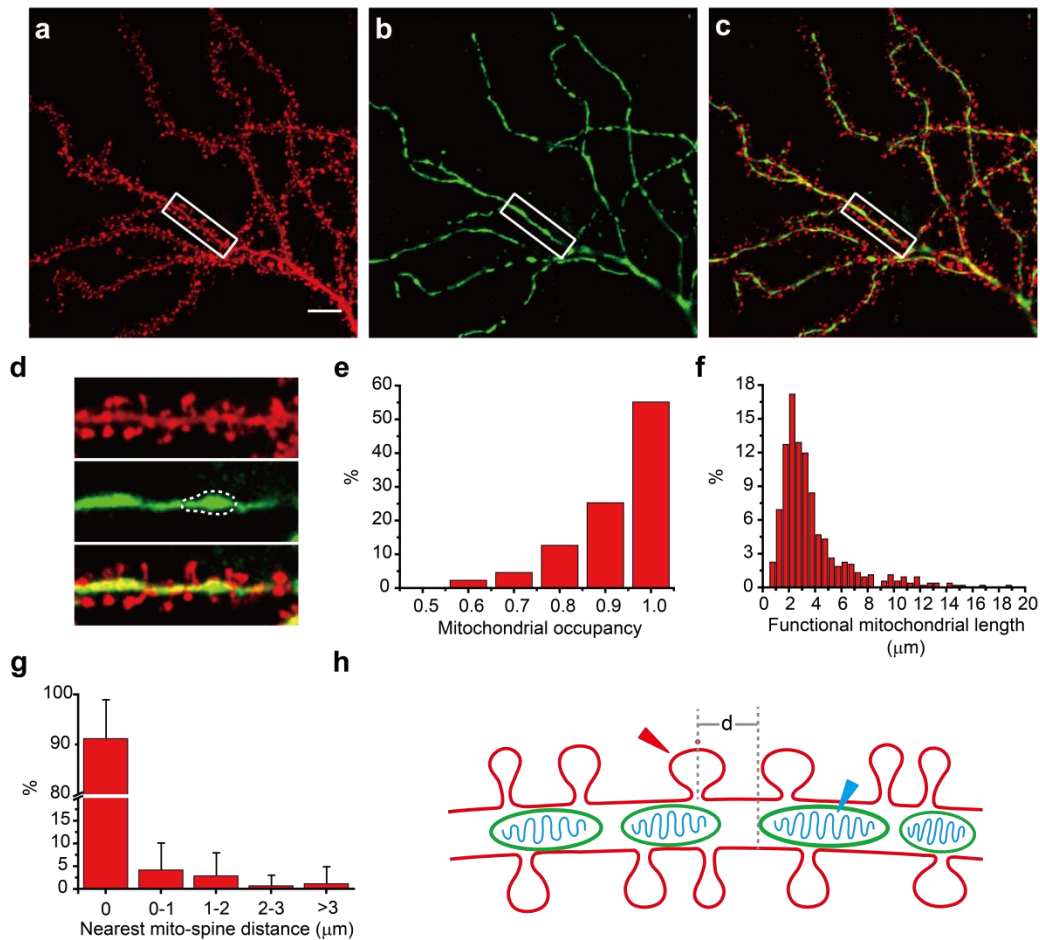
File Name: Supplementary Information

Description: Supplementary Figures and Supplementary Table

File Name: Supplementary Movie 1

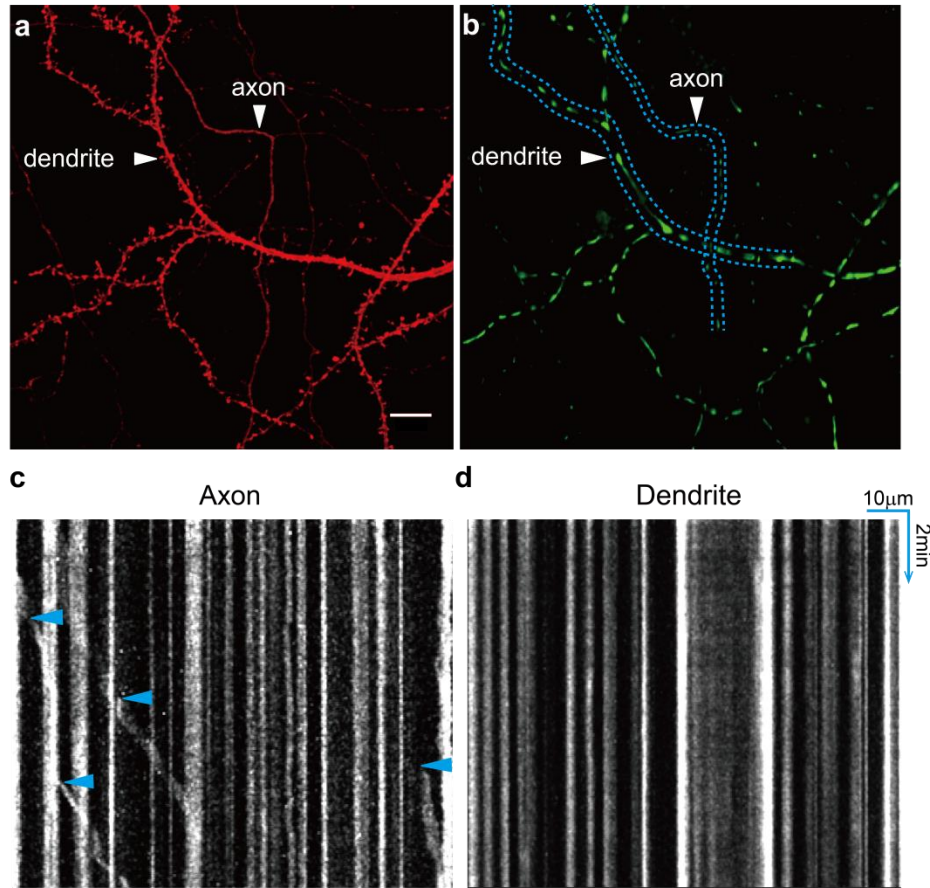
Description: **Dendritic mitoflashes in a primary hippocampal neuron.** Dendritic mitochondria (green) and spines (red) are imaged in a DIV 18 neuron co-expressing mt-cpYFP and actin-mCherry. The movie contains 94 time points at 7.83s intervals. For each time point, the red channel is the maximal intensity projection of a z-stack of 6 mCherry images at 1- μ m axial interval, whereas the green channel displays single mt-cpYFP image at a pre-selected focal plane. Arrowheads are added to indicate the onset of subsequent mitoflashes. Time-courses of these mitoflashes are simultaneously plotted on the right.

Supplementary Figures



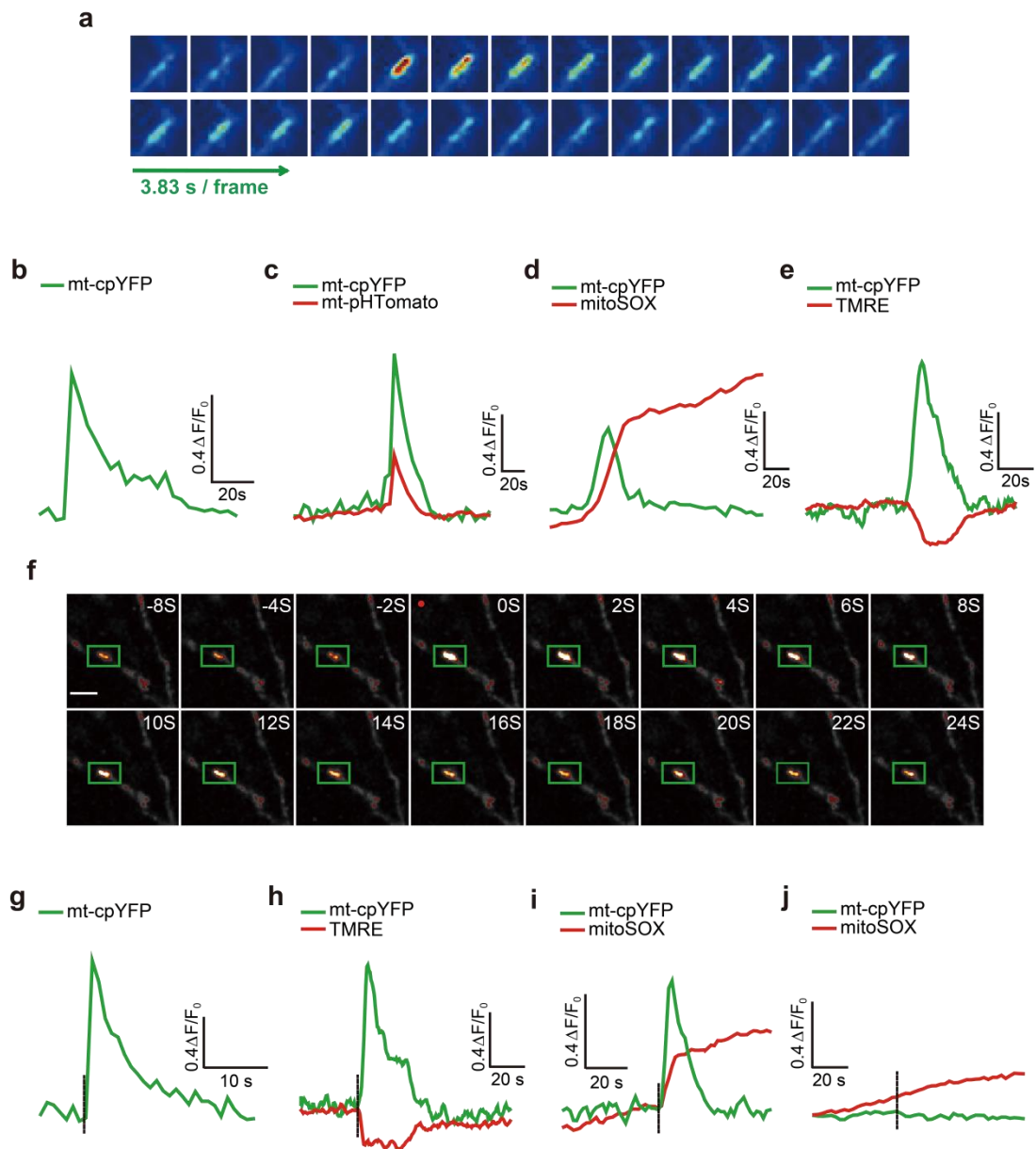
Supplementary Figure 1 Distribution of mitochondria in dendrites.

(a-c) Fluorescence images of dendrites (a) and dendritic mitochondria (b) visualized by actin-mCherry (a) and mt-cpYFP (b). Scale bar, 10 μm . (c) The merged image of (a) and (b). (d) Enlarged views of the boxed regions in (a-c). Dashed line outlines the boundary of a functional mitochondrion based on the spatial extent of a mitoflash. (e) Distribution of mitochondrial occupancy in dendrites. *Mitochondrial occupancy* = $\frac{\text{dendritic mitochondrial length}}{\text{dendritic segment length}}$. The dendrite between two adjacent branch points was considered to be a dendritic segment. n = 151 segments from 17 neurons. (f) Distribution of dendritic mitoflash length. n = 573 mitoflashes, the spatial extent of which reflect the length of functional mitochondria. (g) Distribution of the distance between a spine and its nearest mitochondrion in the parent dendrite (mean \pm s.e.m.). Data are from 20 neurons. (h) Diagram defining the distance between target spine and stimulated mitochondrion. "d" is the distance between target spine neck and nearest edge of stimulated mitochondrion.



Supplementary Figure 2 Mitochondria are stationary in dendrites but mobile in axons.

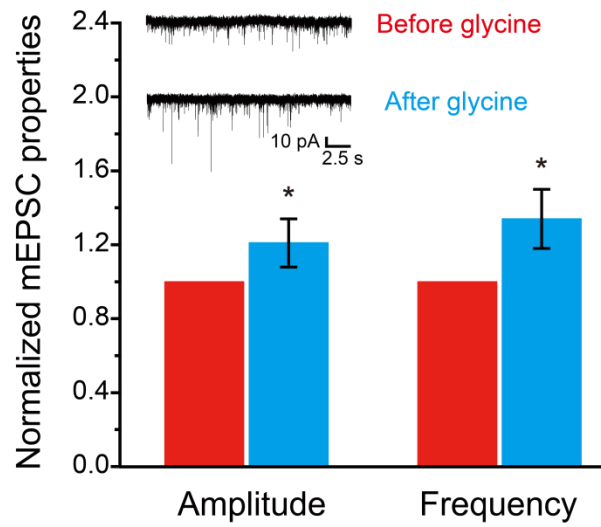
(a) Dendrites and an axon visualized by actin-mCherry, Scale bar, 10 μm . (b) Mitochondria in the dendrites and axon visualized by mt-cpYFP. Dashed lines mark a 100- μm dendrite and a 100- μm axon. Note that axonal mitochondria are generally smaller and dimmer than those in dendrites. (c, d) Kymographs showing mitochondrial movement in an axon (c) and a dendrite (d) within 10 min. Blue triangles point to moving mitochondria.



Supplementary Figure 3 Properties of spontaneous and PA-induced mitoflashes in hippocampal neurons.

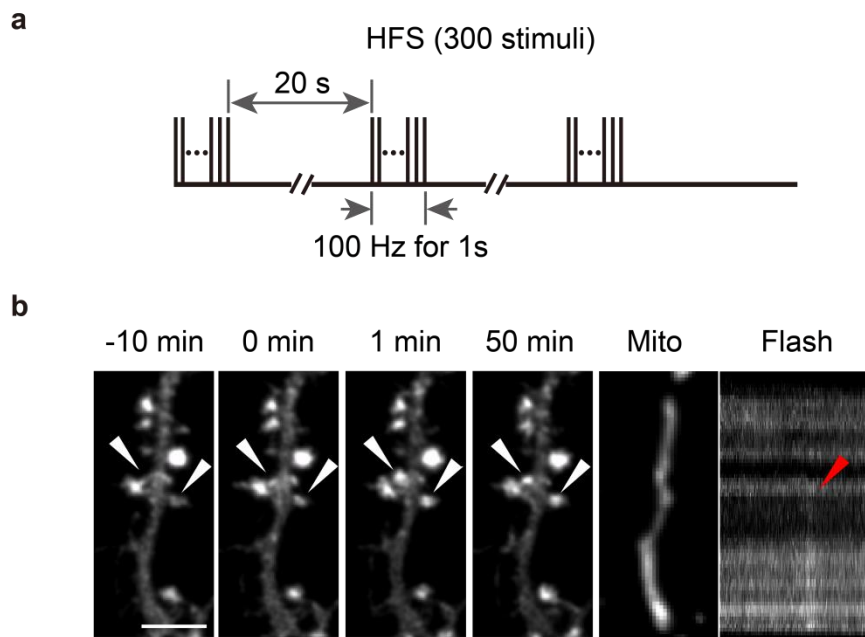
(a-e) Properties of spontaneous mitoflashes in hippocampal neurons. (a) Time-lapse images of a dendritic mitoflash reported by mt-cpYFP and displayed at 3.83 s intervals. Horizontal side length = 5.4 μ m. (b) Time course of the mitoflash in (a). (c) Mitoflash activity is accompanied by pH alkalization reported by mt-pHTomato, a mitochondrion-located pH-sensitive fluorescent protein. (d) The rising phase of the mitoflash is coupled with a step-increase of the mitoSOX signal. (e) Mitoflash is coupled with transient mitochondrial depolarization reported as a decreasing tetramethylrhodamine, ethyl ester (TMRE) signal. In all panels, similar results were obtained in at least 20 experiments. (f-j) Properties of PA-mitoflashes in hippocampal

neurons. **(f)** Time-lapse images of a PA-mitoflash. Green box: target mitochondrion for photoactivation. Red dot denotes the time point for photoactivation. Scale bar, 5 μm . **(g)** Time course of the PA-mitoflash in **(f)**. Vertical dashed line: time of laser stimulation (720 nm at 10 mW for 1 ms). **(h)** PA-mitoflash is coupled with transient depolarization of the mitochondrial membrane potential as measured with TMRE. **(i)** PA-mitoflash is coupled with a stepwise increase of the mitoSOX signal. **(j)** Laser stimulation *per se* does not increase mitoSOX signal when it fails to elicit a PA-mitoflash. Vertical dashed line marks laser stimulation. See also (Supplementary Fig. 7).



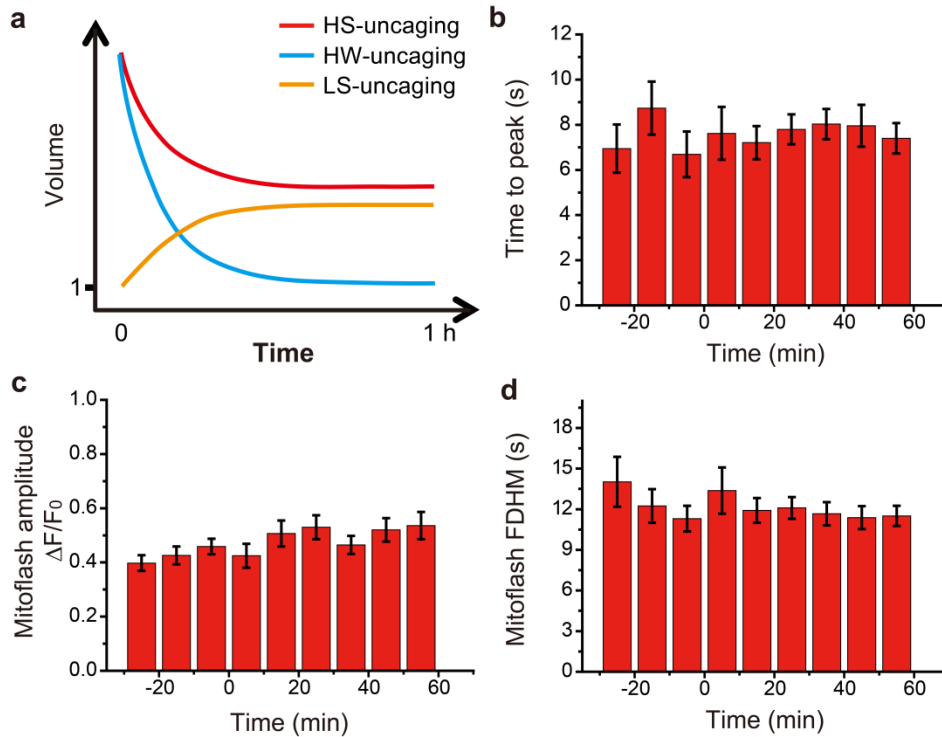
Supplementary Figure 4 Chemical LTP induced by glycine stimulation.

Bars show statistical analysis of changes in mEPSC amplitude and frequency. Insets are examples of electrophysiological recordings before and after 5 min stimulation with 100 μ M glycine. Detailed experimental conditions are described in Methods. $n = 9$ neurons for 5 batches (results are presented as mean \pm s.d.). * $p < 0.05$; paired t-test vs baseline.



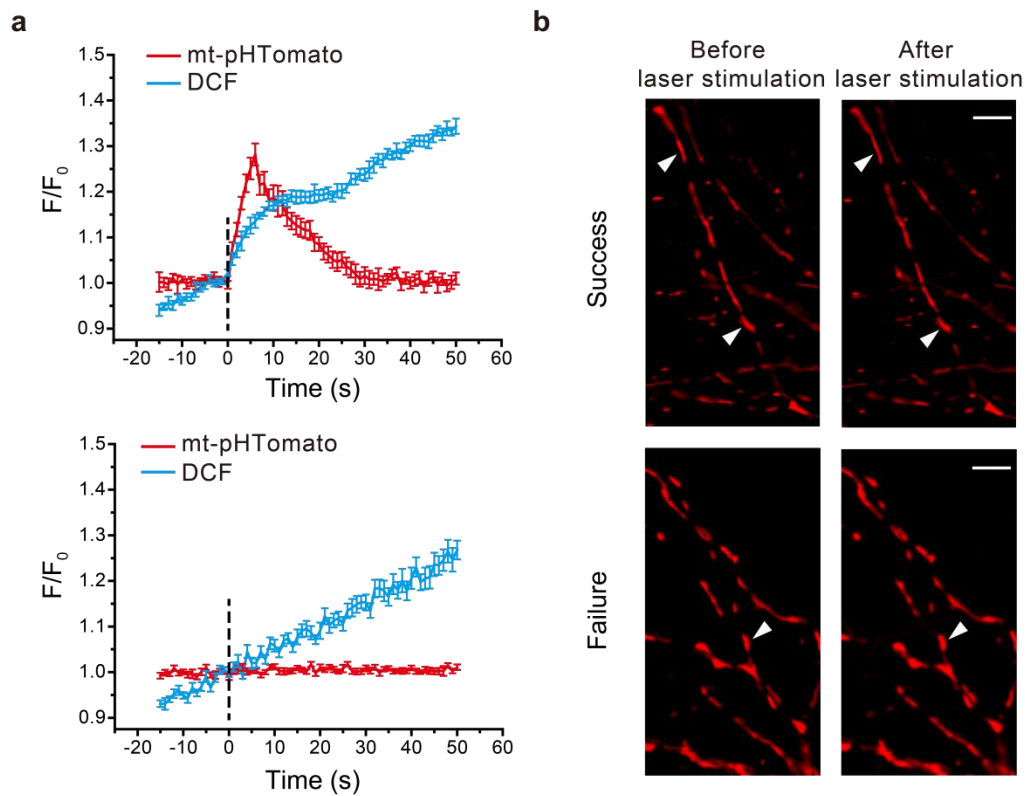
Supplementary Figure 5 Structural LTP induction by high frequency field stimulation.

(a) High frequency field stimulation (HFS) paradigm for induction of sLTP. 3 X 100 pulses at 100Hz, 20s apart. (b) Dendritic segment and mitochondria (Mito) were visualized by actin-mCherry and mt-cpYFP, respectively. Time-lapse images showing spine morphological changes following HFS. Rightmost kymograph was reconstructed along a line on the mitochondrion and corresponds to the period of 10-20min after HFS. White and red arrowheads mark, respectively, spines undergoing sLTP and a mitoflash occurring beneath them. Scale bar, 5 μ m.



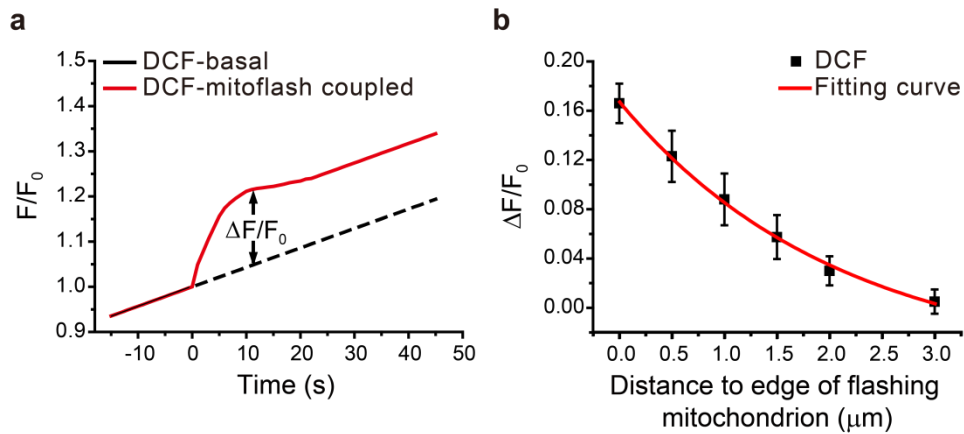
Supplementary Figure 6 Single-spine targeted glutamate uncaging induces CaMKII-dependent sLTP and phasic activation of mitoflashes.

(a) Schematic of the different glutamate-uncaging paradigms. Red, high-concentration strong glutamate-uncaging (HS-uncaging, 6 mM NMI-glutamate, 720 nm laser at 10 mW, 120 pulses, 2 Hz) induced both short-term (<30 min) and long-term spine enlargement. Blue, high-concentration weak stimulation (HW-uncaging, 6 mM NMI-glutamate, 720 nm laser at 10 mW, 40 pulses, 2 Hz) induced only short-term but not long-term spine enlargement. Yellow, low-concentration strong stimulation (LS-uncaging, 2 mM NMI-glutamate, 720 nm laser at 10 mW, 120 pulses, 2 Hz) induced long-term but not short-term spine enlargement. **(b-d)** Properties of individual mitoflashes remained unchanged before and after glutamate uncaging. Data correspond to the experiments reported in Figure 2e. **(b)** Time-to-peak; **(c)** Amplitude; **(d)** Duration, indexed by full duration at half-maximum. $n = 21-56$ mitoflash events per bin. Error bars are SEM.



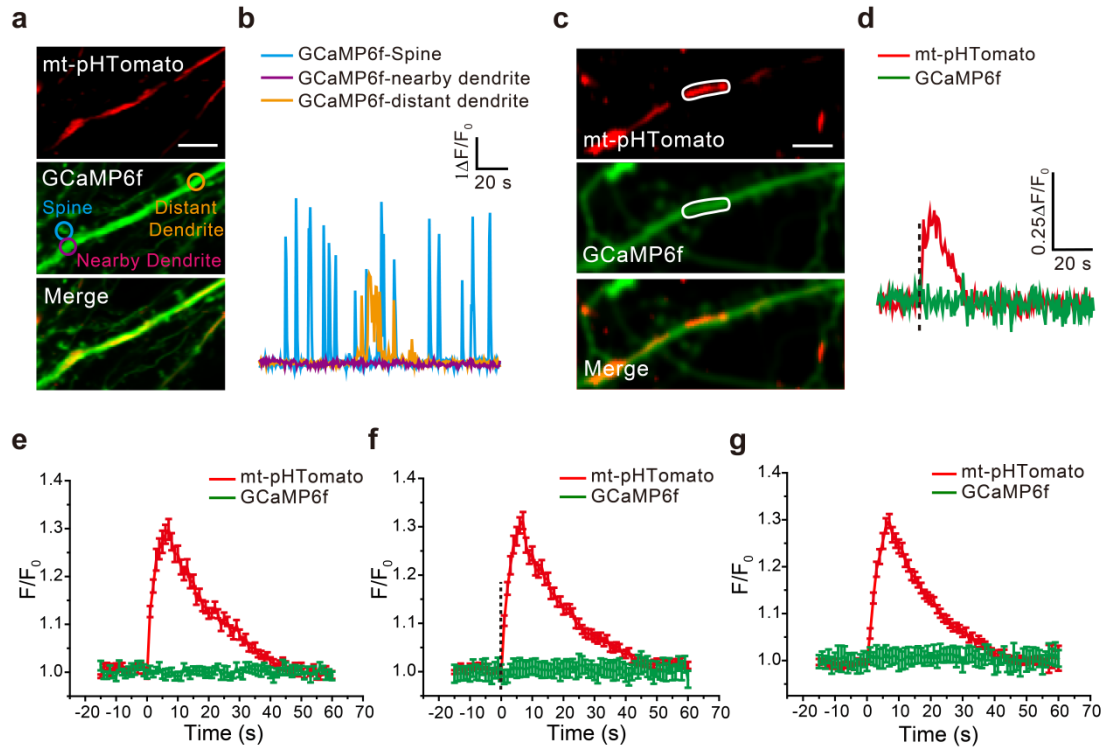
Supplementary Figure 7 Laser stimulation *per se* does not increase local ROS or impair mitochondria during the photoactivation of mitoflash.

(a) Local DCF signal change in response to laser stimulation with (upper panel) and without (lower panel) PA-mitoflashes (reported by mt-pHTomato) (mean \pm s.e.m.). Note that the DCF signals associated with PA-mitoflashes are almost identical to those of spontaneous mitoflashes (Fig 5b). Note also the lack of any stepwise change in the DCF signal when same laser stimulation failed to activate a mitoflash. Vertical dashed line denotes the time of laser stimulation (720 nm, 10mW, 1ms). n= 54 successes and 59 failures. (b) Dendritic mitochondrial morphology (revealed by mt-pHTomato) before and after laser stimulation with and without mitoflash activation. White arrowheads mark target mitochondria. Scale bar, 5 μ m.



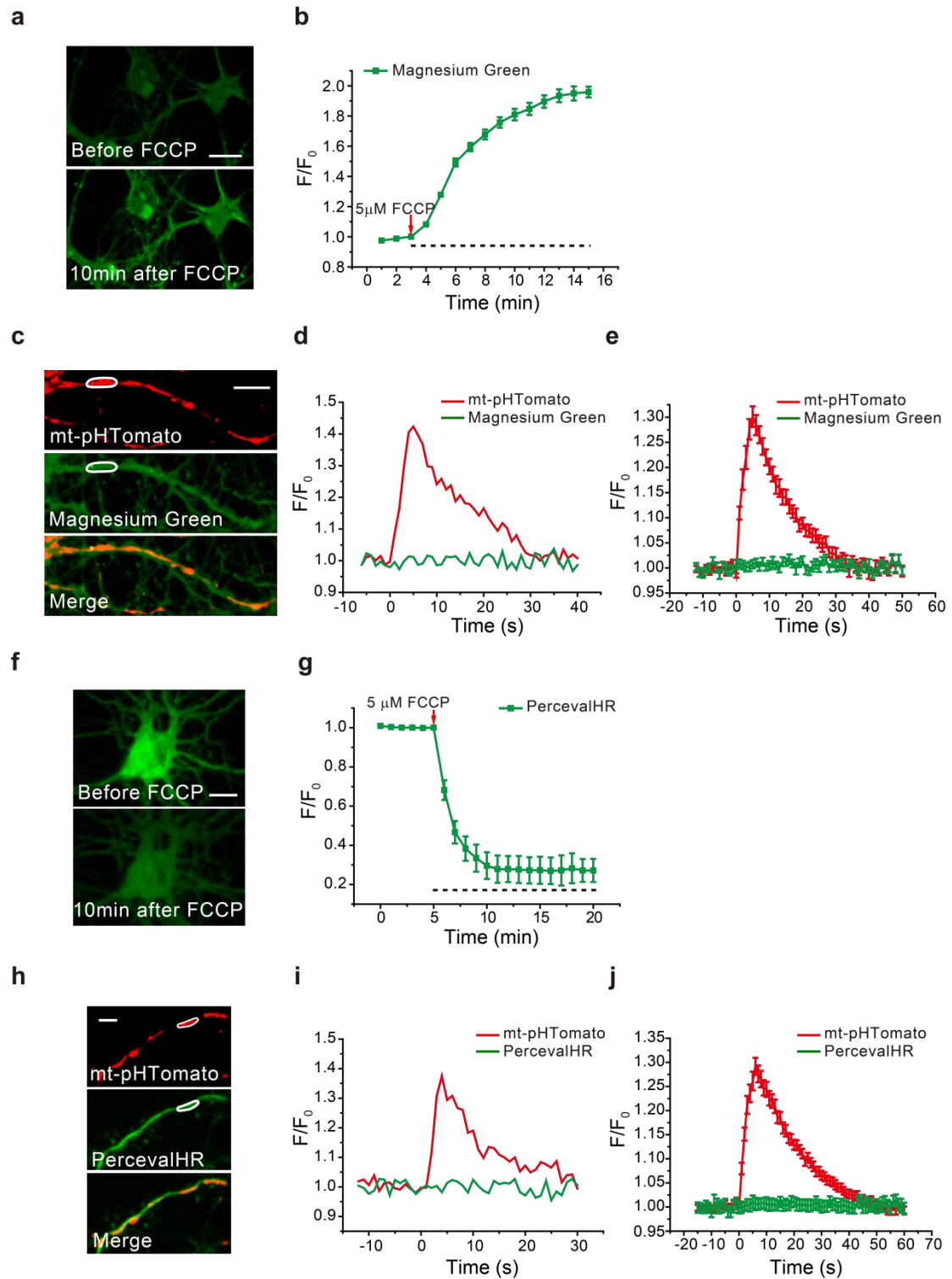
Supplementary Figure 8 Cytosolic ROS signals from flashing mitochondria.

(a) Schematic diagram showing DCF signals associated with mitoflashes, quantified as ($\Delta F/F_0 = DCF_{coupled\ with\ mitoflash} - DCF_{baseline}$). (b) Amplitude of local DCF signal (peak $\Delta F/F_0$) as a function of the distance from the near end of the corresponding mitoflash. A single-exponential fitting (smooth line) yielded a spatial decay constant of $2.07\ \mu\text{m}$ (mean \pm s.e.m.) ($r^2=0.99$).



Supplementary Figure 9 Lack of local cytosolic calcium change associated with dendritic mitoflashes.

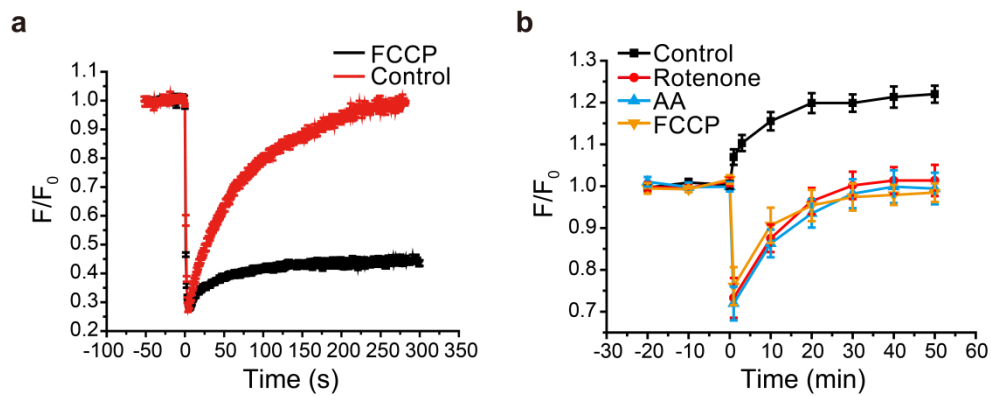
(a) Simultaneous imaging of dendritic mitoflashes (reported by mt-pHTomato) and cytosolic calcium (reported by GCaMP6f). Scale bar, 5 μ m. (b) Spontaneous spine and dendritic calcium transients reported by GCaMP6f. Traces were obtained from a single spine, its nearby dendritic area, and a distant dendritic area, as marked by circles in (a). (c, d) Representative example showing that a dendritic PA-mitoflash does not evoke any detectable change in local cytosolic calcium. White circles in (c) delimit a region of interest encompassing the target mitochondrion. Scale bar, 5 μ m. Dashed line in (d) indicates the time of laser stimulation. (e-g) Average time courses of local dendritic calcium changes during spontaneous (e), photo-activated (f), and nigericin-induced (g) mitoflashes (mean \pm s.e.m.). n= 88, 76, and 131mitoflashes, respectively.



Supplementary Figure 10 Spontaneous mitoflash is not accompanied by any changes in local cytosolic ATP concentration.

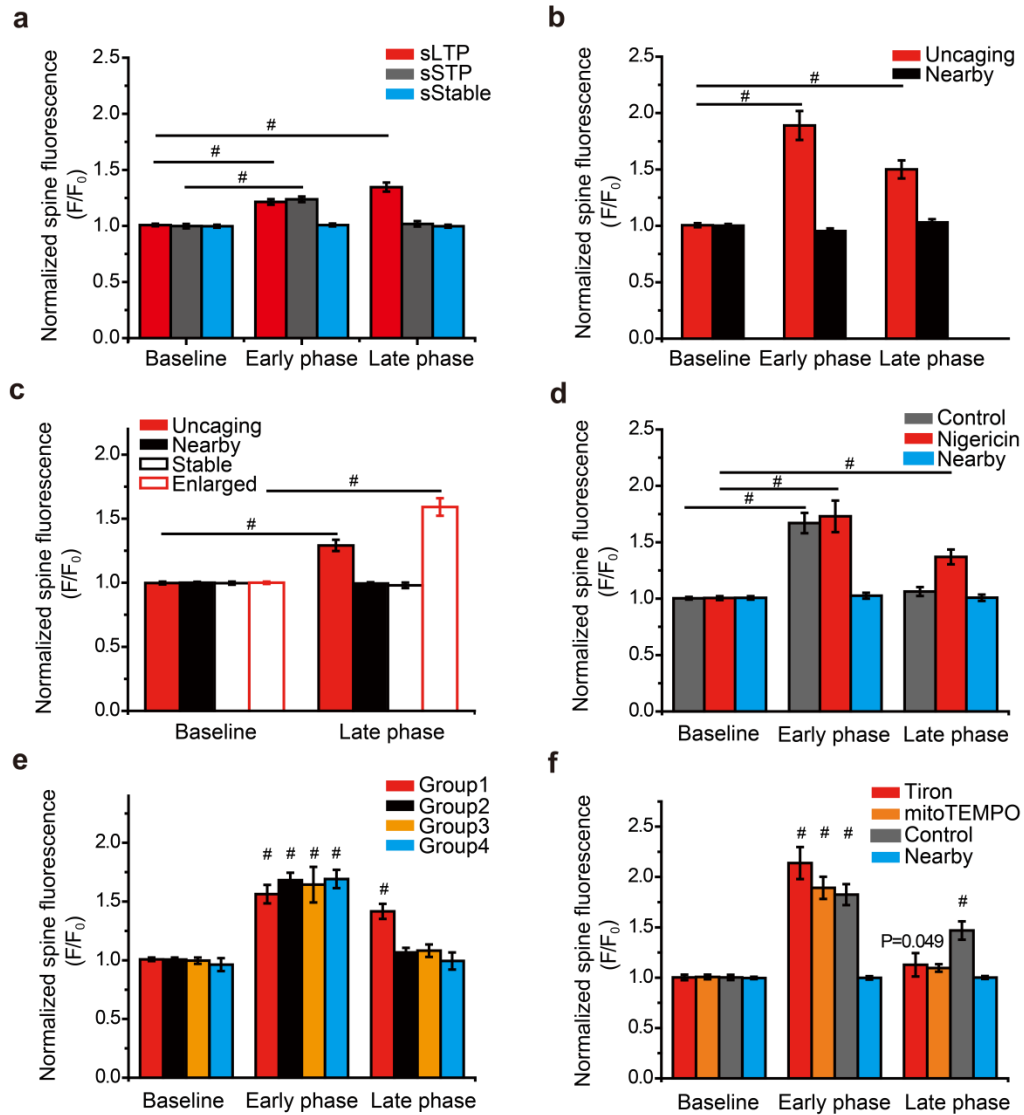
(a) Representative images of magnesium green fluorescence in neurons before and after FCCP (5 μ M)-induced ATP depletion. Scale bar, 10 μ m. (b) Time course of magnesium green signal change during FCCP stimulation. An increase in magnesium

green fluorescence reflects a decrease in ATP concentration, the latter gives rise to an increase in free magnesium concentration (mean \pm s.e.m.). n=33 neurons from 2 batches. **(c)** Representative images showing dendritic mitochondria and cytosolic magnesium green signal. Scale bar, 5 μ m. **(d)** Time courses of a spontaneous mitoflash reported by mt-pHTomato (circled in **c**) and its companion magnesium green signal. **(e)** Statistics. n=117 events in 24 neurons from 3 batches. **(f)** Representative images of percevalHR before and after FCCP (5 μ m) induced ATP depletion in neurons (mean \pm s.e.m.). Scale bar, 10 μ m. **(g)** Time course of percevalHR signal change during FCCP stimulation. Decrease of percevalHR signal (488nm excitation) indicates decrease of cytosolic ATP concentration (mean \pm s.e.m.). n=9 neurons from 3 batches. **(h)** Representative images of dendritic mitochondria and percevalHR signal. Scale bar, 5 μ m. **(i)** Time courses of a mt-pHTomato detected mitoflash (circled in **h**) and accompanying cytosolic percevalHR signal. **(j)** Statistics (mean \pm s.e.m.). n=84 mitoflashes in 12 neurons from 3 batches.



Supplementary Figure 11 ETC inhibitors and the oxidative phosphorylation uncoupler disrupt spine actin dynamics and abolish spine sLTP.

(a) Fluorescence recovery of actin-mcherry after photobleaching (FRAP) shows spine actin dynamics with and without FCCP treatment (20min, 300nM) (mean \pm s.e.m.). (b) Time-dependent spine morphology changes in response to LS glutamate uncaging stimulation with and without ETC and oxidative phosphorylation inhibitors (mean \pm s.e.m.).



Supplementary Figure 12 Statistics of spine size changes as in Figures 1, 2, 4, 5.

(a) Size changes after HFS as in (Figure 1h). The baseline is the averaged normalized spine fluorescence before HFS. The early phase is the averaged spine fluorescence (normalized) at 1 min and 3 min. The late phase is the averaged spine fluorescence (normalized) 30 min after HFS. $n = 8$ neurons from 4 batches. (b) Size changes after HS-glutamate uncaging as in (Figure 2d). The baseline is the averaged normalized spine fluorescence before HS-glutamate uncaging. The early phase is the averaged spine fluorescence (normalized) at 1 min and 3 min. The late phase is the averaged spine fluorescence (normalized) 30 min after glutamate uncaging. (c) Long-term size changes after LS-glutamate uncaging as in (Figure 2g). (d) Size changes after HW-glutamate uncaging as in (Figure 4b). (e) Size changes after HW-glutamate uncaging as in (Figure 4f). (f) Size changes after HS-glutamate uncaging as in (Figure 5d). Error bars are SEM; # $P < 0.001$ (paired sample t-test, early/late phase vs baseline).

Supplementary Table

Supplementary Table 1 Parameters of dendritic mitoflashes under different conditions.

Mitoflash genesis	Time to peak	$\Delta F/F_0$	FDHM
Spontaneous	7.61 ± 0.45 s	0.47 ± 0.02	12.96 ± 0.57 s
Photoactivated	6.78 ± 0.27 s	0.49 ± 0.02	12.89 ± 0.47 s
Nigericin-induced	6.85 ± 0.20 s	0.48 ± 0.01	13.02 ± 0.34 s

Data are mean ± s.e.m.; 500–900 mitoflash events were analyzed for each condition.
FDHM: full duration at half maximum.